

OASIS: Conditional Distribution Shaping for Offline Safe Reinforcement Learning

Yihang Yao^{*1}, Zhepeng Cen^{*1}, Wenhao Ding¹, Haohong Lin¹, Shiqi Liu¹,
Tingnan Zhang², Wenhao Yu², Ding Zhao¹

¹ Carnegie Mellon University, ² Google DeepMind

^{*} Equal contribution, {yihangya, zcen}@andrew.cmu.edu

Abstract

Offline safe reinforcement learning (RL) aims to train a policy that satisfies constraints using a pre-collected dataset. Most current methods struggle with the mismatch between imperfect demonstrations and the desired safe and rewarding performance. In this paper, we introduce OASIS (cOnditionAl diStribution Shaping), a new paradigm in offline safe RL designed to overcome these critical limitations. OASIS utilizes a conditional diffusion model to synthesize offline datasets, thus shaping the data distribution toward a beneficial target domain. Our approach makes compliance with safety constraints through effective data utilization and regularization techniques to benefit offline safe RL training. Comprehensive evaluations on public benchmarks and varying datasets showcase OASIS’s superiority in benefiting offline safe RL agents to achieve high-reward behavior while satisfying the safety constraints, outperforming established baselines. Furthermore, OASIS exhibits high data efficiency and robustness, making it suitable for real-world applications, particularly in tasks where safety is imperative and high-quality demonstrations are scarce.

1 Introduction

Offline Reinforcement Learning (RL), which aims to learn high-reward behaviors from a pre-collected dataset [1, 2], has emerged as a powerful paradigm for handling sequential decision-making tasks such as autonomous driving [3, 4, 5, 6], robotics [7, 8, 9, 10], and control systems [11]. Although standard offline RL has achieved remarkable success in some environments, many real-world tasks cannot be adequately addressed by simply maximizing a scalar reward function due to the existence of various safety constraints that limit feasible solutions. The requirement for *safety*, or constraint satisfaction, is particularly crucial in RL algorithms when deployed in real-world tasks [12, 13, 14, 15, 16, 17, 18].

To develop an optimal policy within a constrained manifold [19, 20], *offline safe RL* has been actively studied in recent years, offering novel ways to integrate safety requirements into offline RL [21]. Existing research in this area incorporates techniques from both offline RL and safe RL, including the use of stationary distribution correction [22, 23], regularization [24, 25], and constrained optimization formulations [26]. Researchers have also proposed the use of sequential modeling methods, such as the decision transformer [27] and the decision diffuser [28, 29] to achieve advantageous policies and meet safety requirements.

Although these methods show promise, it is difficult to handle state-action pairs that are absent from the dataset, which is known notably as out-of-distribution (OOD) extrapolation issues [29, 30, 31]. To solve this, many works utilize regularization methods to push the policy toward behavior policy to achieve pessimism [30, 31]. However, this approach worsens the situation when the dataset is imbalanced and biased: regularization by imperfect demonstrations such as datasets composed predominantly of low-reward data or containing few safe trajectories collected using

unsafe behavior policies. This regularization also leads to another challenge: striking the optimal balance between learning objectives such as task utility efficiency and safety requirements, leading to reward degradation or aggressive behavior [27, 32, 33].

To address these challenges, we introduce a new paradigm in offline safe RL, OASIS (cOnditional AI diStribution Shaping), which steers the offline data distribution to a beneficial target domain using a conditional diffusion model as shown in Figure 1. OASIS distills knowledge from the imperfect dataset, and generates rewarding and safe data according to the cost limit to benefit offline safe RL training. This approach is designed to be compatible with general Q-learning-based offline safe RL algorithms. The key contributions are summarized as follows.

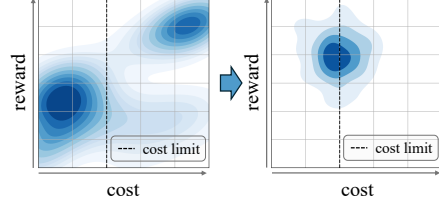


Figure 1: An example of distribution shaping in offline safe RL. We generate a low-cost and high-reward dataset from the original dataset for subsequent RL training.

1. Identification of the safe dataset mismatch (SDM) problem in offline safe RL. We identify the mismatch between the behavior policy and the target policy and investigate the underlying reasons for performance degradation with this condition.

2. Introduction of the OASIS method to address the SDM problem. To the best of our knowledge, this is the first successful application of a distribution shaping paradigm within offline safe RL. Our theoretical analysis further provides insights into performance improvement and safety guarantees.

3. A comprehensive evaluation of our method across various offline safe RL tasks. The experiment results demonstrate that OASIS outperforms baseline methods in terms of both safety and task efficiency for varying tasks and datasets.

2 Related Work

Offline RL. Offline RL addresses the limitations of traditional RL, which requires interaction with the environment. The key literature on offline RL includes BCQ [30], which mitigates the extrapolation error using a generative model, and CQL [34], which penalizes the overestimation of Q-values for unseen actions. BEAR [35] further addresses the extrapolation error by constraining the learned policy to stay close to the behavior policy. OptiDICE [23] directly estimates the stationary distribution corrections of the optimal policy, and COptiDICE [22] extends the method to the constrained RL setting. Recent advances have increasingly focused on the use of data generation to improve policy learning. S4RL [36] shows that surprisingly simple augmentations can dramatically improve policy performance. [37] explores leveraging unlabeled data to improve policy robustness, while [38] proposes survival instincts to enhance agent performance in challenging environments. Counterfactual data augmentation is another promising direction in offline RL [39, 40, 41, 42], highlighting the potential of data generation to significantly improve efficiency and effectiveness.

Safe RL. Safe RL is formulated as a constrained optimization to maximize reward performance while satisfying the pre-defined safety constraint [19, 43, 44, 45, 46, 47, 48]. Primal-dual framework is one common approach to solve safe RL problem [49, 50, 51, 52, 53, 54, 55, 56]. To mitigate the instability issue during online training, [57] proposes PID-based Lagrangian update while [58] and [59] apply variational inference to compute optimal multiplier directly. Another line of work for safe RL is to extend to offline settings, which learn from a fixed dataset to achieve both high reward and constraint satisfaction [60, 61]. [25, 62, 63, 64] tailor online primal-dual-style algorithms to reduce the out-of-distribution issue in offline setting. [27, 65] use decision transformer [66] to avoid the value estimation and exhibit consistent performances across various tasks.

Diffusion Models for RL. Diffusion models have recently gained attention in RL for their capabilities in planning and data generation [67, 68, 69]. Specifically, Diffuser [70] uses a diffusion process to plan the entire trajectory in complex environments. [71] extends this with the Decision Diffuser, which conditions the diffusion process on specific goals and rewards to improve decision-making. SafeDiffuser [72] and FISOR [29] enhance safety by ensuring the planned trajectories satisfying constraints. Combined with the data augmentation capability of diffusion models, AdaptDiffuser [73] achieves state-of-the-art results on offline RL benchmarks. [74] proposes Synthetic Experience Replay, leveraging diffusion models to create synthetic experiences for more efficient learning. [75] demonstrates that diffusion models are effective planners and data synthesizers for multi-task RL,

showcasing their versatility and efficiency. In this work, we investigate the power of diffusion models for safe RL, where the balance between reward and cost presents further complexities.

3 Problem Formulation

3.1 Safe RL with Constrained Markov Decision Process

We formulate Safe RL problems under the Constrained Markov Decision Process (CMDP) framework [76]. A CMDP \mathcal{M} is defined by the tuple $(\mathcal{S}, \mathcal{A}, \mathcal{P}, r, c, \gamma, \mu_0)$, where $\mathcal{S} \in \mathbb{R}^m$ is the state space, $\mathcal{A} \in \mathbb{R}^n$ is the action space, $\mathcal{P} : \mathcal{S} \times \mathcal{A} \times \mathcal{S} \rightarrow [0, 1]$ is the transition function, $r : \mathcal{S} \times \mathcal{A} \times \mathcal{S} \rightarrow \mathbb{R}$ is the reward function, $c : \mathcal{S} \times \mathcal{A} \times \mathcal{S} \rightarrow \mathbb{R}_{\geq 0}$ is the cost function, γ is the discount factor, and $\mu_0 : \mathcal{S} \rightarrow [0, 1]$ is the initial state distribution. Note that this work can also be applied to multiple-constraint tasks, but we use a single-constraint setting for easy demonstration. A safe RL problem is specified by a CMDP and a constraint threshold $\kappa \in [0, +\infty)$. Denote $\pi \in \Pi : \mathcal{S} \times \mathcal{A} \rightarrow [0, 1]$ as the policy and $\tau = \{(s_1, a_1, r_1, c_1), (s_2, a_2, r_2, c_2), \dots\}$ as the trajectory. The stationary state-action distribution under the policy π is defined as $d^\pi(s, a) = (1 - \gamma) \sum_t \gamma^t \Pr(s_t = s, a_t = a)$. The reward and cost returns are defined as $R(\tau) = \sum_\tau r$, and $C(\tau) = \sum_\tau c$. The value function is $V_f^\pi(\mu_0) = \mathbb{E}_{\tau \sim \pi, s_0 \sim \mu_0} [\sum_{t=0}^{\infty} \gamma^t f_t]$, $f \in \{r, c\}$, which is the expectation of discounted return under the policy π and the initial state distribution μ_0 . The goal of safe RL is to find the optimal policy π^* that maximizes the expectation of reward return while constraining the expectation of cost return to the threshold κ :

$$\pi^* = \arg \max_{\pi} \mathbb{E}_{\tau \sim \pi} [R(\tau)], \quad s.t. \quad \mathbb{E}_{\tau \sim \pi} [C(\tau)] \leq \kappa. \quad (1)$$

3.2 Regularized offline safe RL

For an offline safe RL problem, the agent can only access a pre-collected dataset $\mathcal{D} = \cup_i \mathcal{D}_i$, where $\mathcal{D}_i \sim \pi_i^B$ is collected by the behavior policy $\pi_i^B \in \Pi^B$. To solve the problem in Eq.(1), we convert the constraint optimization problem into an unconstrained form:

$$(\pi^*, \lambda^*) = \arg \max_{\lambda} \min_{\pi} \mathcal{J}(\pi, \lambda), \quad \mathcal{J}(\pi, \lambda) = -\mathbb{E}_{\tau \sim \pi} R(\tau) + \lambda(\mathbb{E}_{\tau \sim \pi} C(\tau) - \kappa). \quad (2)$$

The primal-dual-based algorithm solves the optimal policy π^* and the dual variable λ^* by updating (π, λ) iteratively [57, 22, 63]. In offline safe RL tasks, a regularization term is usually introduced to prevent the action OOD issue [77], that is, the objective is converted to:

$$(\pi^*, \lambda^*) = \arg \max_{\lambda} \min_{\pi} \mathcal{J}_{\text{off}}(\pi, \lambda), \quad \mathcal{J}_{\text{off}}(\pi, \lambda) = \mathcal{J}(\pi, \lambda) + wL(\pi, \pi^B), \quad (3)$$

where $w > 0$ is a constant weight, $L(\pi, \pi^B)$ is a regularization term and π^B is the empirical behavior policy and can be viewed as a mixture of $\{\pi_i^B\}$. Practically, regularization is formulated as the MSE regularization [78] or the evidence lower bound regularization [30, 35]. In offline safe RL, there are two main challenges: (1) **Distribution shift** [24]. The agent has poor generalizability when facing OOD state-action pairs during online evaluation; and (2) **Efficiency-safety performance balancing** [27]. The agent tends to be over-conservative or aggressive when taking an over-estimation or an under-estimation of the safety requirements.

4 Method

In this section, we first identify the *safe dataset mismatch* (SDM) problem, which leads to performance degradation when solving the regularized offline safe RL objective (3). Then we present the proposed OASIS (cOnditionAl diStributIon Shaping) method to solve this problem. The OASIS method utilizes the diffusion model to realize conditional distribution shaping, solving the challenges mentioned above, thus benefiting offline safe RL training. Following the proposed algorithm, we provide a theoretical guarantee of the safety performance of the policy learned in this paradigm.

4.1 Identification of the Safe Dataset Mismatch Problem

The regularized offline safe RL objective (3) pushes policy to behavior policy to prevent action OOD issues [31]. When given an imperfect dataset, the state-action distribution deviates from the optimal distribution, and the SDM problem arises: if the behavior policy is too conservative with low costs and low rewards, it leads to task efficiency degradation; if the behavior policy is too aggressive with

high costs and high rewards, it leads to safety violations. To further investigate the SDM problem and the effect of dataset distribution on offline safe RL, we define the **tempting dataset** and **conservative dataset**, which are based on tempting and conservative policies:

Definition 1 (Tempting policy [45] and conservative policy). The tempting policy class is defined as the set of policies that have a higher reward return expectation than the optimal policy, and the conservative policy class is defined as the set of policies that have lower reward and cost return expectations than the optimal policy:

$$\Pi^T := \{\pi : V_r^\pi(\mu_0) > V_r^{\pi^*}(\mu_0)\}, \quad \Pi^C := \{\pi : V_r^\pi(\mu_0) < V_r^{\pi^*}(\mu_0), V_c^\pi(\mu_0) < V_c^{\pi^*}(\mu_0)\}. \quad (4)$$

Intuitively, a tempting policy is a more rewarding but less safe policy than the optimal one, and a conservative policy is with lower cost but less rewarding. According to these policies, we define two types of datasets:

Definition 2 (Tempting and conservative dataset). For an offline dataset $D_i \sim \pi_i$, if $\pi_i \in \Pi^B \cap \Pi^T$, then the dataset is tempting; if $\pi_i \in \Pi^B \cap \Pi^C$, then the dataset is conservative.

Staying within the tempting dataset distribution results in tempting (unsafe) behavior, while staying within the conservative dataset distribution causes reward degradation. A theoretical analysis of performance degradation due to the SDM problem is presented in section 4.4. Figure 2 illustrates examples of both conservative and tempting datasets. It is important to note that tempting and conservative datasets are prevalent in offline safe RL since optimal policies are rarely available for data collection. The SDM problem is a distinct feature of offline safe RL, indicating that training the policy on either tempting or conservative datasets will violate safety constraints or result in sub-optimality, both of which are undesirable. Therefore, addressing the SDM problem is essential for the development of regularized offline safe RL algorithms.

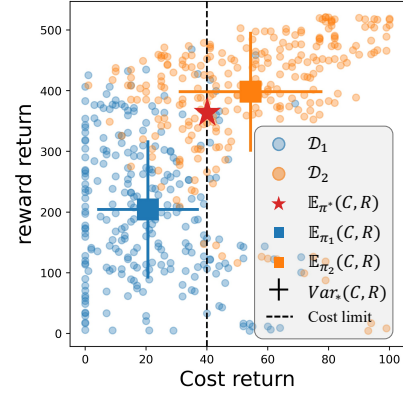


Figure 2: D_1 is a conservative dataset, and D_2 is a tempting dataset. Each point represents $(C(\tau), R(\tau))$ of a trajectory τ in the dataset.

4.2 Mitigating the Safe Dataset Mismatch

We propose to use the distribution shaping of the dataset to mitigate the SDM problem, that is, generating a new dataset D_g by reshaping the original data distribution. As shown in Figure 1, the key idea is to adjust the dataset distribution towards the optimal distribution under π^* , reducing the distribution discrepancy and mitigating the SDM problem, thus solving the action OOD issue and efficiency-safety balancing problem simultaneously.

Dataset reweighting, which assigns different sampling weights to different data points, is a straightforward way to do distribution shaping [33, 79]. In the offline RL domain, researchers proposed methods to assign high weights to data that achieve high rewards and superior performance in many RL tasks [33, 79]. To validate this idea, we deploy a Boltzmann energy function considering both the reward and the cost for the reweighting strategy to solve the problem (see Appendix B for details). The experimental results, shown in Figure 3, validate the effectiveness of this distribution shaping method when the coverage of the dataset is complete.

However, for a more general case where we can only access the low-quality dataset (e.g., tempting datasets in Figure 3), simply performing data reweighting does not work well due to the absence of

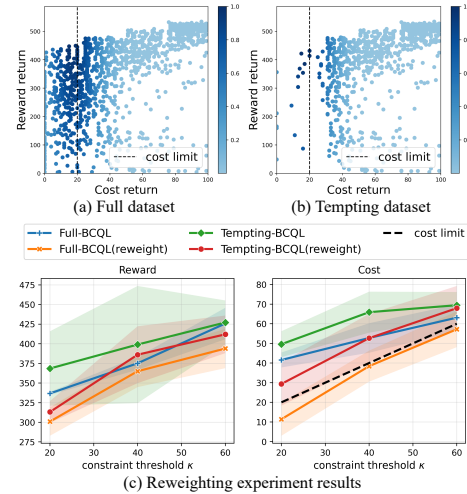


Figure 3: (a) Reweighting in the dataset with comprehensive coverage. (b) Reweighting in the tempting dataset. (c) Performance evaluation with different weights and datasets.

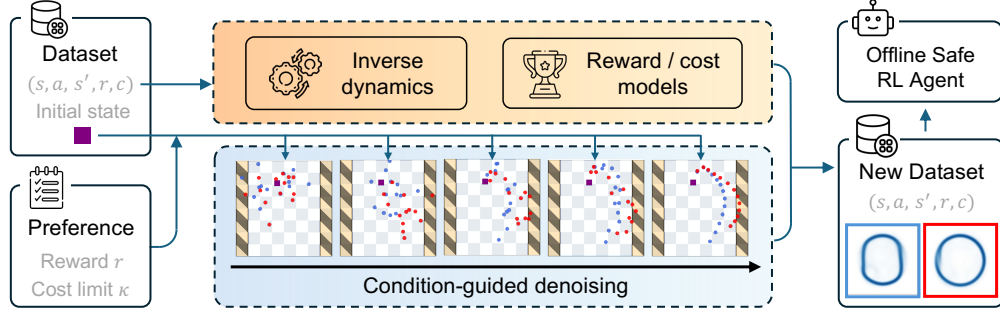


Figure 4: OASIS overview.

necessary data. Thus, we propose to use a conditional generative model for more flexible distribution shaping, which generates new data by stitching sub-optimal trajectories for offline training.

4.3 Constraint-Conditioned Diffusion Model as Data Generator

To overcome the limitation of reweighing methods, we propose using diffusion models to generate the dataset that fits the target cost limit to achieve distribution shaping. In the following, we introduce the details of the training and generation phases.

Training. In previous works [73, 70], the trajectory planning in offline RL can be viewed as the sequential data generation: $\tau = [s_0, s_1, \dots, s_{L-1}]$, where τ is a subsequence of trajectory with length L . Denote $\mathbf{x}_k(\tau)$ and $\mathbf{y}(\tau)$ as the k -step denoising output of the diffusion model and the denoising conditions such as reward and cost returns, respectively. Then the forward diffusion process is to add noise to $\mathbf{x}_k(\tau)$ and gradually convert it into Gaussian noise:

$$q(\mathbf{x}_k(\tau) | \mathbf{x}_{k-1}(\tau)) := \mathcal{N}(\mathbf{x}_k(\tau); \sqrt{1 - \beta_k} \mathbf{x}_{k-1}(\tau), \beta_k \mathbf{I}), \quad k = 1, \dots, K \quad (5)$$

where β_k is a pre-defined beta schedule, K is the total denoising timestep. Then the trainable denoising step aims at gradually converting the Gaussian noise back to a valid trajectory:

$$p_\theta(\mathbf{x}_{k-1}(\tau) | \mathbf{x}_k(\tau), \mathbf{y}(\tau)) := \mathcal{N}(\mathbf{x}_{k-1}(\tau) | \mu_\theta(\mathbf{x}_k(\tau), \mathbf{y}(\tau), k), \Sigma_k), \quad (6)$$

where θ is the trainable parameter. We use a simplified surrogate loss [80] for optimization:

$$\mathcal{L}_{\text{denoise}} := \mathbb{E}_{\mathbf{x}_0(\tau) \sim q, \epsilon \sim \mathcal{N}(\mathbf{0}, \mathbf{I})} [\|\epsilon - \epsilon_\theta(\mathbf{x}_k(\tau), \mathbf{y}(\tau), k)\|^2]. \quad (7)$$

In this work, we use the classifier-free guidance [81] for conditional data generation. The condition $\mathbf{y}(\tau)$ in (6) and (7) is set to $\mathbf{y}(\tau) = [\hat{C}(\tau), \hat{R}(\tau)]$. Thus, the denoising process depends on the target reward and cost returns of the planned subtrajectory. During training time, the diffusion model learns both an unconditional denoising core $\epsilon_\theta(\mathbf{x}_k(\tau), \emptyset, k)$ and a conditional denoising core $\epsilon_\theta(\mathbf{x}_k(\tau), \mathbf{y}(\tau), k)$. We adopt masking [71] for the training to zero out the condition of one training trajectory and categorize it as the \emptyset class with probability $0 < p < 1$. Within the given raw dataset, we also train an inverse dynamics model $\hat{f}: \mathcal{S} \times \mathcal{S} \rightarrow \mathcal{A}$, and reward and cost models $\hat{r}(s, a, s'), \hat{c}(s, a, s'): \mathcal{S} \times \mathcal{A} \times \mathcal{S} \rightarrow \mathbb{R}$ for labeling.

Generation. After obtaining a trained model, the next step is to generate a new dataset following the conditions. For diffusion model inference, the denoising core $\epsilon_\theta(\mathbf{x}_k(\tau), \mathbf{y}, k)$ is calculated by:

$$\epsilon_\theta(\mathbf{x}_k(\tau), \mathbf{y}(\tau), k) = \epsilon_\theta(\mathbf{x}_k(\tau), \emptyset, k) + w_\alpha (\epsilon_\theta(\mathbf{x}_k(\tau), \mathbf{y}_c(\tau), k) - \epsilon_\theta(\mathbf{x}_k(\tau), \emptyset, k)), \quad (8)$$

where $w_\alpha > 0$ is a constant guidance scale and $\mathbf{y}_c := [\hat{C}, \hat{R}]$ is the generation condition. In practice, condition \hat{C} is determined by the cost threshold κ , and condition \hat{R} is selected based on the raw data distribution. It should be noticed that for guided generation, we fix the initial state, which means that we replace the initial state of each k -step noised trajectory as $\mathbf{x}_k[0] = \mathbf{x}_0[0]$.

After generating one subtrajectory $\tau_g = \mathbf{x}_0$, we can get the state and action sequence $s_g = \tau_g[: -1]$, $s'_g = \tau_g[1 :]$, $a_g = \hat{f}(s_g, s'_g)$, then label the data $r_g = \hat{r}(s_g, a_g, s'_g)$, $c_g = \hat{c}(s_g, a_g, s'_g)$. Finally, we get a generated dataset $\mathcal{D}_g = \{s_g, a_g, s'_g, r_g, c_g\}$ with $|\tau_g| - 1$ transition pairs. With this new dataset, we can further train offline safe RL agents.

In this work, we consider BCQ-Lag [30, 57] as the base offline safe RL algorithm. The process of generating one subtrajectory τ_g is summarized in Alg. 1. More details of the implementation are available in Appendix C.

4.4 Theoretical analysis

We first investigate how the distribution mismatch degrades the policy performance on constraint satisfaction. Suppose that the maximum one-step cost is $C_{\max} = \max_{s,a} c(s,a)$. Based on Lemma 6 in [82] and Lemma 2 in [83], the performance gap between the policy π learned with the dataset \mathcal{D} and the optimal policy is bounded by

$$|V_c^\pi(\mu_0) - V_c^*(\mu_0)| \leq \frac{2C_{\max}}{1-\gamma} D_{\text{TV}}(d^\mathcal{D}(s) \| d^*(s)) + \frac{2C_{\max}}{1-\gamma} \mathbb{E}_{d^*(s)} [D_{\text{TV}}(\pi(a|s) \| \pi^*(a|s))], \quad (9)$$

where $d^\mathcal{D}(s), d^*(s)$ denote the stationary state distribution of the dataset and optimal policy. The proof is given in Appendix A.1. Therefore, a significant mismatch between the dataset and the optimal policy results in both a substantial state distribution TV distance and a large policy shift from the optimal one, which can cause notable performance degradation, especially when the offline RL algorithm enforces the learned policy to closely resemble the behavior policy of the offline data.

Then we provide a theoretical analysis of how our method mitigates this mismatch issue by shrinking the distribution gap, which provides a guarantee of the safety performance of the regularized offline safe RL policy. Let $d_g(s|\mathbf{y})$ denote the state marginal of the generated data with condition \mathbf{y} . We first make the following assumptions.

Assumption 1 (Score estimation error of the state marginal). There exists a condition \mathbf{y}^* such that the score function error of the state marginal is bounded by

$$\mathbb{E}_{d^*(s)} \|\nabla_s \log d_g(s|\mathbf{y}^*) - \nabla_s \log d^*(s)\| \leq \varepsilon_{\text{score}}^2, \quad (10)$$

where $d^*(s)$ is the stationary state distribution induced by the optimal policy π^* .

This assumption is also adopted in previous work [84, 85]. For simplicity, we omit the condition \mathbf{y}^* in the following analysis and use $d_g(s), d_g(s,a)$ to denote the generated state or the state-action distribution with condition \mathbf{y}^* . As we use inverse dynamics $f(a|s, s')$ to calculate actions based on the generated state sequence, the quality of the dataset is also determined by the inverse dynamics. Therefore, we further make the following assumption.

Assumption 2 (Error of inverse policy). The error of action distribution generated by the inverse dynamics is bounded by

$$\mathbb{E}_{d^*(s)} [D_{\text{KL}}(\hat{\pi}_{\text{inv}}(\cdot|s) \| \pi^*(\cdot|s))] \leq \varepsilon_{\text{inv}}, \quad (11)$$

where $\hat{\pi}_{\text{inv}}(a|s) = \mathbb{E}_{s'} [\hat{f}(a|s, s')]$ denotes the empirical inverse policy, which is a marginal of inverse dynamics over s' .

Then the distance of generated data distribution to the optimal one is bounded as:

Theorem 1 (Distribution shaping error bound). *Suppose that the optimal stationary state distribution satisfies that 1) its score function $\nabla_s \log d^*(s)$ is L -Lipschitz and 2) its second momentum is bounded. Under Assumption 1 and 2, the gap of generated state-action distribution to the optimal stationary state-action distribution is bounded by*

$$D_{\text{TV}}(d_g(s,a) \| d^*(s,a)) \leq \tilde{\mathcal{O}}\left(\varepsilon_{\text{score}} \sqrt{K}\right) + \sqrt{\varepsilon_{\text{inv}}/2} + C(d^*(s), L, K), \quad (12)$$

where $C(d^*(s), L, K)$ represents a constant determined by $d^*(s), L$ and K .

The proof is given in Appendix A.2. Theorem 1 indicates that using the proposed OASIS method, we can shape the dataset distribution towards a bounded neighborhood of the optimal distribution.

Algorithm 1: OASIS (generation)

Input: Raw dataset \mathcal{D} , constraint threshold

κ

Output: Generated sub-trajectory τ_g

- 1: Sample a initial state: $s \sim \mathcal{D}$
 - 2: Get initial noisy sub-trajectory:
 $x_k = [s, s_1, \dots, s_{L-1}], s_i \sim \mathcal{N}(\mathbf{0}, \mathbf{I})$
 - 3: Determine the condition \mathbf{y}_c ;
 - 4: **for** $k = K, \dots, 1$ **do**
 - 5: Calculate $\epsilon(x_k, \mathbf{y}_c, k)$ (8);
 - 6: Inverse sampling state x_{k-1} (6)
 - 7: **end for**
 - 8: Get actions, rewards, and costs from x_0 ;
 - 9: **Return:** trajectory τ_g
-

Given the generated data, we will then train a regularized offline safe RL policy by (3). Notice that the regularization term in the objective function in (3) is equivalent to an explicit policy constraint, and the coefficient w is the corresponding dual variable. Therefore, we make the following assumption on the distance between the learned policy π_ϕ and the behavior policy.

Assumption 3. Denote the generated dataset as \mathcal{D}_g and the corresponding behavior policy as π_g , given a fixed coefficient w , for the policy π_ϕ optimized by (3), there exists a ε_{reg} such that

$$\mathbb{E}_{d_g(s)} [D_{\text{KL}}(\pi_\phi(\cdot|s) \parallel \pi_g(\cdot|s))] \leq \varepsilon_{\text{reg}}. \quad (13)$$

Based on the above assumptions, we can derive the bound of constraint violation of the policy learned on the offline data generated by OASIS. The proof is given in Appendix A.3.

Theorem 2 (Constraint violation bound). *For policy π_ϕ optimized by regularized-based offline safe RL on generated dataset \mathcal{D}_g , under assumption 1, 2 and 3, the constraint violation of the trained policy is bounded as:*

$$V_c^{\pi_\phi}(\mu_0) - \kappa \leq \frac{2C_{\max}}{1-\gamma} \left(\tilde{O}(\varepsilon_{\text{score}}\sqrt{K}) + C(d^*(s), L, K) + \sqrt{\varepsilon_{\text{inv}}/2} + \sqrt{\varepsilon_{\text{reg}}/2} \right), \quad (14)$$

where $C(d^*(s), L, K)$ represents a constant determined by $d^*(s)$, L and K .

5 Experiment

In the experiments, we answer these questions: (1) How does the distribution of the dataset influence the performance of regularized offline safe RL? (2) How does our proposed distribution shaping method perform in offline safe RL tasks? (3) How well does the conditional data generator shape the dataset distribution? To address these questions, we set up the following experiment tasks.

Environments. We adopt the continuous robot locomotion control tasks in the public benchmark Bullet-Safety-Gym [86] for evaluation, which is commonly used in previous works [65, 27, 53]. We consider two tasks, Run and Circle, and three types of robots, Ball, Car, and Drone. We name the environment as Agent-Task. A detailed description is available in the Appendix B.

Datasets. Our experiment tasks are mainly built upon the offline safe RL dataset OSRL [87]. To better evaluate the tested algorithms with the challenging SDM problem, we create four different training dataset types, full, tempting, conservative, and hybrid. The tempting dataset contains sparse safe demonstrations, the conservative dataset lacks rewarding data points, and the hybrid dataset has scarcity in the medium-reward, medium-cost trajectories. We set different cost thresholds for different datasets. A detailed description and visualization of the datasets are available in Appendix B.

Table 1: Evaluation results of the normalized reward and cost. The cost threshold is 1. \uparrow : the higher the reward, the better. \downarrow : the lower the cost (up to threshold 1), the better. **Blue**: Safe agents whose normalized cost is smaller than 1. Gray: Unsafe agents. **Blue**: Safe agent with the highest reward.

Algorithm	Stats	Tasks					
		BallRun	CarRun	DroneRun	BallCircle	CarCircle	DroneCircle
BC	reward \uparrow	0.55 \pm 0.23	0.94 \pm 0.02	0.62 \pm 0.11	0.73 \pm 0.05	0.59 \pm 0.11	0.82 \pm 0.01
	cost \downarrow	2.04 \pm 1.32	1.50 \pm 1.11	3.48 \pm 0.68	2.53 \pm 0.15	3.39 \pm 0.85	3.29 \pm 0.18
CPQ	reward \uparrow	0.25 \pm 0.11	0.63 \pm 0.51	0.13 \pm 0.30	0.39 \pm 0.34	0.64 \pm 0.02	0.01 \pm 0.02
	cost \downarrow	1.34 \pm 1.32	1.43 \pm 1.82	2.29 \pm 1.98	0.73 \pm 0.66	0.12 \pm 0.19	3.16 \pm 3.85
COptiDICE	reward \uparrow	0.63 \pm 0.04	0.90 \pm 0.03	0.71 \pm 0.01	0.73 \pm 0.02	0.52 \pm 0.01	0.35 \pm 0.02
	cost \downarrow	3.13 \pm 0.17	0.28 \pm 0.24	3.87 \pm 0.08	2.83 \pm 0.23	3.56 \pm 0.16	0.12 \pm 0.10
BEAR-Lag	reward \uparrow	0.65 \pm 0.08	0.55 \pm 0.62	0.10 \pm 0.33	0.89 \pm 0.02	0.80 \pm 0.08	0.89 \pm 0.04
	cost \downarrow	4.38 \pm 0.28	8.44 \pm 0.62	3.72 \pm 3.22	2.84 \pm 0.28	2.89 \pm 0.84	4.03 \pm 0.51
BCQ-Lag	reward \uparrow	0.51 \pm 0.19	0.96 \pm 0.06	0.76 \pm 0.07	0.76 \pm 0.04	0.79 \pm 0.02	0.88 \pm 0.04
	cost \downarrow	1.96 \pm 0.88	2.31 \pm 3.22	5.19 \pm 1.08	2.62 \pm 0.29	3.25 \pm 0.28	3.90 \pm 0.55
CDT	reward \uparrow	0.35 \pm 0.01	0.96 \pm 0.01	0.84 \pm 0.12	0.73 \pm 0.01	0.71 \pm 0.01	0.17 \pm 0.08
	cost \downarrow	1.56 \pm 1.10	0.67 \pm 0.03	7.56 \pm 0.33	1.36 \pm 0.03	2.39 \pm 0.15	1.08 \pm 0.62
FISOR	reward \uparrow	0.17 \pm 0.03	0.85 \pm 0.02	0.44 \pm 0.14	0.28 \pm 0.03	0.24 \pm 0.05	0.49 \pm 0.05
	cost \downarrow	0.04 \pm 0.06	0.15 \pm 0.20	2.52 \pm 0.61	0.00 \pm 0.00	0.15 \pm 0.27	0.02 \pm 0.03
CVAE-BCQL	reward \uparrow	0.25 \pm 0.02	0.88 \pm 0.00	0.21 \pm 52.07	0.49 \pm 0.03	0.60 \pm 0.05	0.01 \pm 0.02
	cost \downarrow	1.40 \pm 0.35	0.00 \pm 0.00	2.80 \pm 0.63	1.39 \pm 0.27	1.77 \pm 0.47	3.31 \pm 1.66
OASIS (ours)	reward \uparrow	0.28 \pm 0.01	0.85 \pm 0.04	0.13 \pm 0.08	0.70 \pm 0.01	0.76 \pm 0.03	0.60 \pm 0.01
	cost \downarrow	0.79 \pm 0.37	0.02 \pm 0.03	0.79 \pm 0.54	0.45 \pm 0.14	0.89 \pm 0.59	0.25 \pm 0.10

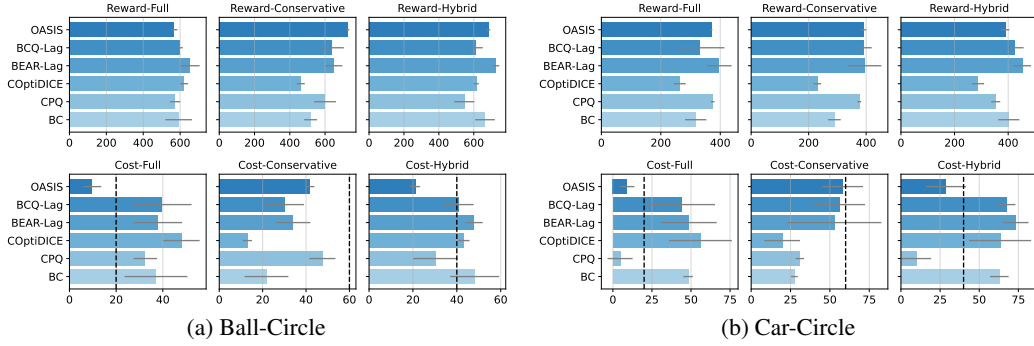


Figure 5: Performance with different datasets and varying constraint thresholds.

Baselines. We compared our method with five types of baseline methods: (1) Q-learning-based algorithms: BCQ-Lag [30, 57], BEAR-Lag [35, 57], and CPQ [25]; (2) Imitation learning: Behavior Cloning (BC) [25]; (3) Distribution correction estimation: COptiDICE [23], and (4) sequential modeling algorithms: CDT [27] and FISOR [29]; (5) Data generate: CVAE-BCQL: we train BCQ-Lag agents on the datasets generated by Conditional Variational Autoencoder (CVAE) [88].

Metrics. We use the normalized cost return and the normalized reward return as the evaluation metric for comparison in Table 1 and 2. The normalized cost is defined as $C_{\text{normalized}} = C_{\pi}/\kappa$, where C_{π} is the cost return and κ is the cost threshold. The agent is safe if $C_{\text{normalized}} \leq 1$. The normalized reward is computed by $R_{\text{normalized}} = R_{\pi}/r_{\max}(\mathcal{M})$, where $r_{\max}(\mathcal{M})$ is the maximum empirical reward return for task \mathcal{M} within the given dataset. We report the averaged results and standard deviations over 3 seeds for all the quantity evaluations.

5.1 How can conditional data generation benefit offline safe RL?

Performance degradation with SDM problems. The comparison results on the tempting dataset are presented in Table. 1 with the cost threshold $\kappa = 20$ before normalization. Results of BC show the mismatch between the behavior policy and the safe policy, as the cost returns significantly violate the safety constraints. The results of BCQ-Lag and BEAR-Lag show this mismatch further influences the regularized-based algorithms, leading to constraint violations. This is because the regularization term pushes the policy towards the unsafe behavior policy. The conservative Q function estimation method CPQ, exhibits a significant reward degradation in all the tested tasks, which arises from the drawback of the pessimistic estimation methods learning over-conservative behaviors. COptiDICE is also not able to learn safe and rewarding policies, showing that even using distribution correction estimation is not enough to solve the SDM problem. For the sequential modeling algorithms, CDT shows poor safety performance and FISOR tends to be over-conservative with poor reward performance. This is because both methods require a large amount of high-quality data while the trajectories with low cost and high reward are sparse in this task. These observations further motivate the distribution shaping for offline safe RL.

Performance improvement using OASIS.

From Table 1, we find that only our method OASIS can learn safe and rewarding policies by mitigating the SDM problem. In addition to the results on the tempting dataset, we also provide evaluation results within different types of datasets and constraint thresholds in Figure 5a and Figure 5b. We can observe that most baselines still fail to learn a safe policy within different task conditions due to the SDM issue. In contrast, our proposed OASIS method achieves the highest reward among all safe agents, which shows strength in more general cases.

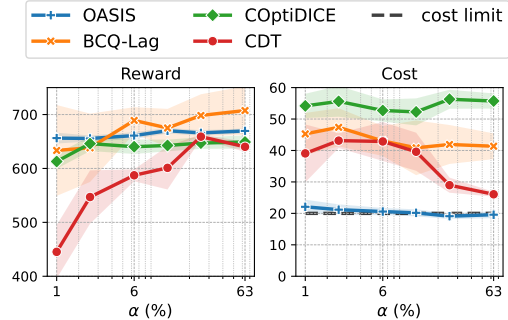


Figure 6: Data efficiency on the Ball-Circle task with a tempting dataset.

High data efficiency of OASIS. We evaluate data efficiency by changing the amount of generated data. Denote α as the amount ratio of the generated data and the raw dataset, the evaluation results are shown in Figure 6, which indicates that we can still learn a good policy using a small amount of high-quality data ($\alpha < 2\%$) generated by OASIS. In contrast, baseline methods show significant performance degradation when the data are sparse as the noisy data is of low quality.

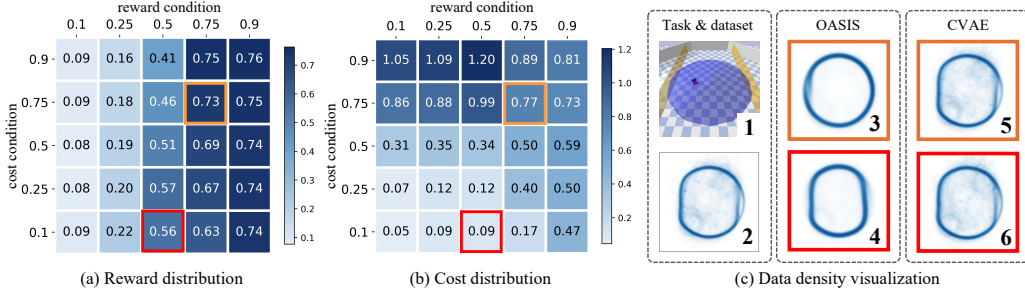


Figure 7: (a)(b) Reward and cost performance of the generated data: $\mathbb{E}[r(s, a)]$, $\mathbb{E}[c(s, a)]$, $(s, a) \sim d_g$. The x-axis and y-axis mean the reward and cost conditions and the values of both conditions and expectations are normalized with the same scale. (c) Visualization of the data density. 1: Car-circle task; 2: The density of the (x, y) position of the raw dataset; 3, 4: The density of the position (x, y) of the data generated by OASIS under conditions $[0.1, 0.5]$ and $[0.75, 0.75]$; 5, 6: the density of the position (x, y) of the data generated by CVAE under conditions $[0.1, 0.5]$ and $[0.75, 0.75]$

5.2 How can OASIS shape the dataset distribution?

Successful distribution shaping. To show the capability of dataset distribution shaping of the proposed OASIS and baseline CVAE, we generate the dataset under different conditions and visualize them in Figure 7. We can first observe that, when using different conditions, the expectations of reward and cost of the generated dataset change accordingly. This shows the strong capability of our method in distribution shaping. We also visualize the density of the generated data. In the Car-circle task, the robot receives high rewards when moving along the circle boundary and receives costs when it exceeds the boundaries on both sides, as shown in Figure 7(c). The original dataset contains trajectories with various safety performances. When using a low-cost condition, the generated data are clustered within the safety boundary to satisfy the constraints. When using a high-reward condition, the generated data points are closer to the circle boundary and receive higher rewards. In contrast, the baseline CVAE cannot successfully incorporate the conditions in data generation, resulting in almost similar datasets with different conditions as shown in Figure 7(c).

5.3 Robust performance against denoising steps

We conduct an ablation study on the key hyperparameter of the proposed OASIS method. The experiment related to the denoising steps K is presented in Table 2. Performance does not change much with different values, which shows the robustness of the proposed OASIS method.

Table 2: Ablation study on denoising step K

K		10	20	40
Ball-	reward	0.71 ± 0.02	0.70 ± 0.01	0.71 ± 0.01
Circle	cost	0.72 ± 0.10	0.45 ± 0.14	0.99 ± 0.13
Ball-	reward	0.29 ± 0.04	0.28 ± 0.01	0.29 ± 0.01
Run	cost	0.16 ± 0.14	0.79 ± 0.37	0.00 ± 0.00

6 Conclusion

In this paper, we study the challenging problem in offline safe RL: the safe data mismatch between the imperfect demonstration and the target performance requirements. To address this issue, we proposed the OASIS method, which utilizes a conditional diffusion model to realize the dataset distribution shaping, benefiting offline safe RL training. In addition to the theoretical guarantee of performance improvement, we also conduct extensive experiments to show the superior performance of OASIS in learning a safe and rewarding policy on many challenging offline safe RL tasks. More importantly, our method shows good data efficiency and robustness to hyperparameters, which makes it preferable for applications in many real-world tasks.

There are two limitations of OASIS: 1) Offline training takes longer: our method involves preprocessing the offline dataset to enhance quality, which requires more time and computing resources; 2) Achieving zero-constraint violations remains challenging with imperfect demonstrations. One potential negative social impact is that misuse of our method may cause harmful consequences and safety issues. Nevertheless, we believe that our proposed method can inspire further research in the safe learning community and help to adapt offline RL algorithms to real-world tasks with safety requirements.

References

- [1] Rafael Figueiredo Prudencio, Marcos ROA Maximo, and Esther Luna Colombini. A survey on offline reinforcement learning: Taxonomy, review, and open problems. *IEEE Transactions on Neural Networks and Learning Systems*, 2023.
- [2] Justin Fu, Aviral Kumar, Ofir Nachum, George Tucker, and Sergey Levine. D4rl: Datasets for deep data-driven reinforcement learning. *arXiv preprint arXiv:2004.07219*, 2020.
- [3] Kyle Stachowicz and Sergey Levine. Racer: Epistemic risk-sensitive rl enables fast driving with fewer crashes. *arXiv preprint arXiv:2405.04714*, 2024.
- [4] Haohong Lin, Wenhao Ding, Zuxin Liu, Yaru Niu, Jiacheng Zhu, Yuming Niu, and Ding Zhao. Safety-aware causal representation for trustworthy offline reinforcement learning in autonomous driving. *IEEE Robotics and Automation Letters*, 2024.
- [5] Zhili Zhang, Songyang Han, Jiangwei Wang, and Fei Miao. Spatial-temporal-aware safe multi-agent reinforcement learning of connected autonomous vehicles in challenging scenarios. In *2023 IEEE International Conference on Robotics and Automation (ICRA)*, pages 5574–5580. IEEE, 2023.
- [6] Xing Fang, Qichao Zhang, Yinfeng Gao, and Dongbin Zhao. Offline reinforcement learning for autonomous driving with real world driving data. In *2022 IEEE 25th International Conference on Intelligent Transportation Systems (ITSC)*, pages 3417–3422. IEEE, 2022.
- [7] Cheng Chi, Siyuan Feng, Yilun Du, Zhenjia Xu, Eric Cousineau, Benjamin Burchfiel, and Shuran Song. Diffusion policy: Visuomotor policy learning via action diffusion. *arXiv preprint arXiv:2303.04137*, 2023.
- [8] Wenhao Ding, Laixi Shi, Yuejie Chi, and Ding Zhao. Seeing is not believing: Robust reinforcement learning against spurious correlation. *Advances in Neural Information Processing Systems*, 36, 2024.
- [9] Weiye Zhao, Rui Chen, Yifan Sun, Ruixuan Liu, Tianhao Wei, and Changliu Liu. Guard: A safe reinforcement learning benchmark. *arXiv preprint arXiv:2305.13681*, 2023.
- [10] Jinning Li, Xinyi Liu, Banghua Zhu, Jiantao Jiao, Masayoshi Tomizuka, Chen Tang, and Wei Zhan. Guided online distillation: Promoting safe reinforcement learning by offline demonstration. *arXiv preprint arXiv:2309.09408*, 2023.
- [11] Xianyu Zhan, Haoran Xu, Yue Zhang, Xiangyu Zhu, Honglei Yin, and Yu Zheng. Deepthermal: Combustion optimization for thermal power generating units using offline reinforcement learning. In *Proceedings of the AAAI Conference on Artificial Intelligence*, volume 36, pages 4680–4688, 2022.
- [12] Dohyeong Kim, Yunho Kim, Kyungjae Lee, and Songhwai Oh. Safety guided policy optimization. In *2022 IEEE/RSJ International Conference on Intelligent Robots and Systems (IROS)*, pages 2462–2467. IEEE, 2022.
- [13] Tairan He, Chong Zhang, Wenli Xiao, Guanqi He, Changliu Liu, and Guanya Shi. Agile but safe: Learning collision-free high-speed legged locomotion. *arXiv preprint arXiv:2401.17583*, 2024.
- [14] Wenli Xiao, Tairan He, John Dolan, and Guanya Shi. Safe deep policy adaptation. *arXiv preprint arXiv:2310.08602*, 2023.
- [15] Weidong Huang, Jiaming Ji, Borong Zhang, Chunhe Xia, and Yaodong Yang. Safedreamer: Safe reinforcement learning with world models. In *The Twelfth International Conference on Learning Representations*, 2023.
- [16] Zhaorun Chen, Binhao Chen, Tairan He, Liang Gong, and Chengliang Liu. Progressive adaptive chance-constrained safeguards for reinforcement learning. *arXiv preprint arXiv:2310.03379*, 2023.
- [17] Wenjun Zou, Yao Lv, Jie Li, Yujie Yang, Shengbo Eben Li, Jingliang Duan, Xianyu Zhan, Jingjing Liu, Yaqin Zhang, and Keqiang Li. Policy bifurcation in safe reinforcement learning. *arXiv preprint arXiv:2403.12847*, 2024.
- [18] Yujie Yang, Yuxuan Jiang, Yichen Liu, Jianyu Chen, and Shengbo Eben Li. Model-free safe reinforcement learning through neural barrier certificate. *IEEE Robotics and Automation Letters*, 8(3):1295–1302, 2023.

- [19] Javier Garcia and Fernando Fernández. A comprehensive survey on safe reinforcement learning. *Journal of Machine Learning Research*, 16(1):1437–1480, 2015.
- [20] Lukas Brunke, Melissa Greeff, Adam W Hall, Zhaocong Yuan, Siqu Zhou, Jacopo Panerati, and Angela P Schoellig. Safe learning in robotics: From learning-based control to safe reinforcement learning. *Annual Review of Control, Robotics, and Autonomous Systems*, 5, 2021.
- [21] Akifumi Wachi, Xun Shen, and Yanan Sui. A survey of constraint formulations in safe reinforcement learning. *arXiv preprint arXiv:2402.02025*, 2024.
- [22] Jongmin Lee, Cosmin Paduraru, Daniel J Mankowitz, Nicolas Heess, Doina Precup, Kee-Eung Kim, and Arthur Guez. Coptidice: Offline constrained reinforcement learning via stationary distribution correction estimation. *arXiv preprint arXiv:2204.08957*, 2022.
- [23] Jongmin Lee, Wonseok Jeon, Byungjun Lee, Joelle Pineau, and Kee-Eung Kim. Optidice: Offline policy optimization via stationary distribution correction estimation. In *International Conference on Machine Learning*, pages 6120–6130. PMLR, 2021.
- [24] Ilya Kostrikov, Rob Fergus, Jonathan Tompson, and Ofir Nachum. Offline reinforcement learning with fisher divergence critic regularization. In *International Conference on Machine Learning*, pages 5774–5783. PMLR, 2021.
- [25] Haoran Xu, Xianyuan Zhan, and Xiangyu Zhu. Constraints penalized q-learning for safe offline reinforcement learning. In *Proceedings of the AAAI Conference on Artificial Intelligence*, volume 36, pages 8753–8760, 2022.
- [26] Hoang Le, Cameron Voloshin, and Yisong Yue. Batch policy learning under constraints. In *International Conference on Machine Learning*, pages 3703–3712. PMLR, 2019.
- [27] Zuxin Liu, Zijian Guo, Yihang Yao, Zhepeng Cen, Wenhao Yu, Tingnan Zhang, and Ding Zhao. Constrained decision transformer for offline safe reinforcement learning. *arXiv preprint arXiv:2302.07351*, 2023.
- [28] Qian Lin, Bo Tang, Zifan Wu, Chao Yu, Shangqin Mao, Qianlong Xie, Xingxing Wang, and Dong Wang. Safe offline reinforcement learning with real-time budget constraints. *arXiv preprint arXiv:2306.00603*, 2023.
- [29] Yinan Zheng, Jianxiong Li, Dongjie Yu, Yujie Yang, Shengbo Eben Li, Xianyuan Zhan, and Jingjing Liu. Safe offline reinforcement learning with feasibility-guided diffusion model. *arXiv preprint arXiv:2401.10700*, 2024.
- [30] Scott Fujimoto, David Meger, and Doina Precup. Off-policy deep reinforcement learning without exploration. In *International conference on machine learning*, pages 2052–2062. PMLR, 2019.
- [31] Laixi Shi, Gen Li, Yuting Wei, Yuxin Chen, and Yuejie Chi. Pessimistic q-learning for offline reinforcement learning: Towards optimal sample complexity. In *International conference on machine learning*, pages 19967–20025. PMLR, 2022.
- [32] Yihang Yao, Zuxin Liu, Zhepeng Cen, Peide Huang, Tingnan Zhang, Wenhao Yu, and Ding Zhao. Gradient shaping for multi-constraint safe reinforcement learning. *arXiv preprint arXiv:2312.15127*, 2023.
- [33] Zhang-Wei Hong, Aviral Kumar, Sathwik Karnik, Abhishek Bhandwadar, Akash Srivastava, Joni Pajarinen, Romain Laroche, Abhishek Gupta, and Pulkit Agrawal. Beyond uniform sampling: Offline reinforcement learning with imbalanced datasets. *Advances in Neural Information Processing Systems*, 36:4985–5009, 2023.
- [34] Aviral Kumar, Aurick Zhou, George Tucker, and Sergey Levine. Conservative q-learning for offline reinforcement learning. *Advances in Neural Information Processing Systems*, 33:1179–1191, 2020.
- [35] Aviral Kumar, Justin Fu, Matthew Soh, George Tucker, and Sergey Levine. Stabilizing off-policy q-learning via bootstrapping error reduction. *Advances in neural information processing systems*, 32, 2019.
- [36] Samarth Sinha, Ajay Mandlekar, and Animesh Garg. S4rl: Surprisingly simple self-supervision for offline reinforcement learning in robotics. In *Conference on Robot Learning*, pages 907–917. PMLR, 2022.

- [37] Tianhe Yu, Aviral Kumar, Yevgen Chebotar, Karol Hausman, Chelsea Finn, and Sergey Levine. How to leverage unlabeled data in offline reinforcement learning. In *International Conference on Machine Learning*, pages 25611–25635. PMLR, 2022.
- [38] Anqi Li, Dipendra Misra, Andrey Kolobov, and Ching-An Cheng. Survival instinct in offline reinforcement learning. *Advances in neural information processing systems*, 36, 2024.
- [39] Silviu Pitis, Elliot Creager, and Animesh Garg. Counterfactual data augmentation using locally factored dynamics. *Advances in Neural Information Processing Systems*, 33:3976–3990, 2020.
- [40] Ahmed Aloui, Juncheng Dong, Cat P Le, and Vahid Tarokh. Counterfactual data augmentation with contrastive learning. *arXiv preprint arXiv:2311.03630*, 2023.
- [41] Chaochao Lu, Biwei Huang, Ke Wang, José Miguel Hernández-Lobato, Kun Zhang, and Bernhard Schölkopf. Sample-efficient reinforcement learning via counterfactual-based data augmentation. *arXiv preprint arXiv:2012.09092*, 2020.
- [42] Silviu Pitis, Elliot Creager, Ajay Mandlekar, and Animesh Garg. Mocoda: Model-based counterfactual data augmentation. *Advances in Neural Information Processing Systems*, 35:18143–18156, 2022.
- [43] Joshua Achiam, David Held, Aviv Tamar, and Pieter Abbeel. Constrained policy optimization. In *International Conference on Machine Learning*, pages 22–31. PMLR, 2017.
- [44] Shangding Gu, Long Yang, Yali Du, Guang Chen, Florian Walter, Jun Wang, Yaodong Yang, and Alois Knoll. A review of safe reinforcement learning: Methods, theory and applications. *arXiv preprint arXiv:2205.10330*, 2022.
- [45] Zuxin Liu, Zijian Guo, Zhepeng Cen, Huan Zhang, Jie Tan, Bo Li, and Ding Zhao. On the robustness of safe reinforcement learning under observational perturbations. *arXiv preprint arXiv:2205.14691*, 2022.
- [46] Dohyeong Kim, Kyungjae Lee, and Songhwai Oh. Trust region-based safe distributional reinforcement learning for multiple constraints. *Advances in neural information processing systems*, 36, 2024.
- [47] Sheng Xu and Guiliang Liu. Uncertainty-aware constraint inference in inverse constrained reinforcement learning. In *The Twelfth International Conference on Learning Representations*, 2023.
- [48] Dohyeong Kim, Mineui Hong, Jeongho Park, and Songhwai Oh. Scale-invariant gradient aggregation for constrained multi-objective reinforcement learning. *arXiv preprint arXiv:2403.00282*, 2024.
- [49] Yinlam Chow, Mohammad Ghavamzadeh, Lucas Janson, and Marco Pavone. Risk-constrained reinforcement learning with percentile risk criteria. *Journal of Machine Learning Research*, 18(167):1–51, 2018.
- [50] Chen Tessler, Daniel J Mankowitz, and Shie Mannor. Reward constrained policy optimization. *arXiv preprint arXiv:1805.11074*, 2018.
- [51] Alex Ray, Joshua Achiam, and Dario Amodei. Benchmarking safe exploration in deep reinforcement learning. *arXiv preprint arXiv:1910.01708*, 7, 2019.
- [52] Dongsheng Ding, Kaiqing Zhang, Tamer Basar, and Mihailo Jovanovic. Natural policy gradient primal-dual method for constrained markov decision processes. *Advances in Neural Information Processing Systems*, 33:8378–8390, 2020.
- [53] Yiming Zhang, Quan Vuong, and Keith Ross. First order constrained optimization in policy space. *Advances in Neural Information Processing Systems*, 2020.
- [54] Zhepeng Cen, Yihang Yao, Zuxin Liu, and Ding Zhao. Feasibility consistent representation learning for safe reinforcement learning. *arXiv preprint arXiv:2405.11718*, 2024.
- [55] Zifan Wu, Bo Tang, Qian Lin, Chao Yu, Shangqin Mao, Qianlong Xie, Xingxing Wang, and Dong Wang. Off-policy primal-dual safe reinforcement learning. *arXiv preprint arXiv:2401.14758*, 2024.
- [56] Dongsheng Ding, Zhengyan Huan, and Alejandro Ribeiro. Resilient constrained reinforcement learning. In *International Conference on Artificial Intelligence and Statistics*, pages 3412–3420. PMLR, 2024.

- [57] Adam Stooke, Joshua Achiam, and Pieter Abbeel. Responsive safety in reinforcement learning by pid lagrangian methods. In *International Conference on Machine Learning*, pages 9133–9143. PMLR, 2020.
- [58] Zuxin Liu, Zhepeng Cen, Vladislav Isenbaev, Wei Liu, Steven Wu, Bo Li, and Ding Zhao. Constrained variational policy optimization for safe reinforcement learning. In *International Conference on Machine Learning*, pages 13644–13668. PMLR, 2022.
- [59] Sandy Huang, Abbas Abdolmaleki, Giulia Vezzani, Philemon Brakel, Daniel J Mankowitz, Michael Neunert, Steven Bohez, Yuval Tassa, Nicolas Heess, Martin Riedmiller, et al. A constrained multi-objective reinforcement learning framework. In *Conference on Robot Learning*, pages 883–893. PMLR, 2022.
- [60] Jiayi Guan, Li Shen, Ao Zhou, Lusong Li, Han Hu, Xiaodong He, Guang Chen, and Changjun Jiang. Poce: Primal policy optimization with conservative estimation for multi-constraint offline reinforcement learning. In *Proceedings of the IEEE/CVF Conference on Computer Vision and Pattern Recognition*, pages 26243–26253, 2024.
- [61] Qin Zhang, Linrui Zhang, Haoran Xu, Li Shen, Bowen Wang, Yongzhe Chang, Xueqian Wang, Bo Yuan, and Dacheng Tao. Saformer: A conditional sequence modeling approach to offline safe reinforcement learning. *arXiv preprint arXiv:2301.12203*, 2023.
- [62] Nicholas Polosky, Bruno C Da Silva, Madalina Fiterau, and Jithin Jagannath. Constrained offline policy optimization. In *International Conference on Machine Learning*, pages 17801–17810. PMLR, 2022.
- [63] Kihyuk Hong, Yuhang Li, and Ambuj Tewari. A primal-dual-critic algorithm for offline constrained reinforcement learning. In *International Conference on Artificial Intelligence and Statistics*, pages 280–288. PMLR, 2024.
- [64] Jiayi Guan, Guang Chen, Jiaming Ji, Long Yang, Zhijun Li, et al. Voce: Variational optimization with conservative estimation for offline safe reinforcement learning. *Advances in Neural Information Processing Systems*, 36, 2024.
- [65] Zijian Guo, Weichao Zhou, and Wenchao Li. Temporal logic specification-conditioned decision transformer for offline safe reinforcement learning. *arXiv preprint arXiv:2402.17217*, 2024.
- [66] Lili Chen, Kevin Lu, Aravind Rajeswaran, Kimin Lee, Aditya Grover, Michael Laskin, Pieter Abbeel, Aravind Srinivas, and Igor Mordatch. Decision transformer: Reinforcement learning via sequence modeling. *arXiv preprint arXiv:2106.01345*, 2021.
- [67] Zhengbang Zhu, Hanye Zhao, Haoran He, Yichao Zhong, Shenyu Zhang, Yong Yu, and Weinan Zhang. Diffusion models for reinforcement learning: A survey. *arXiv preprint arXiv:2311.01223*, 2023.
- [68] Jaewoo Lee, Sujin Yun, Taeyoung Yun, and Jinkyoo Park. Gta: Generative trajectory augmentation with guidance for offline reinforcement learning. *arXiv preprint arXiv:2405.16907*, 2024.
- [69] Hui Yuan, Kaixuan Huang, Chengzhuo Ni, Minshuo Chen, and Mengdi Wang. Reward-directed conditional diffusion: Provable distribution estimation and reward improvement. *Advances in Neural Information Processing Systems*, 36, 2024.
- [70] Michael Janner, Yilun Du, Joshua B Tenenbaum, and Sergey Levine. Planning with diffusion for flexible behavior synthesis. *arXiv preprint arXiv:2205.09991*, 2022.
- [71] Anurag Ajay, Yilun Du, Abhi Gupta, Joshua Tenenbaum, Tommi Jaakkola, and Pulkit Agrawal. Is conditional generative modeling all you need for decision-making? *arXiv preprint arXiv:2211.15657*, 2022.
- [72] Wei Xiao, Tsun-Hsuan Wang, Chuang Gan, and Daniela Rus. Safediffuser: Safe planning with diffusion probabilistic models. *arXiv preprint arXiv:2306.00148*, 2023.
- [73] Zhixuan Liang, Yao Mu, Mingyu Ding, Fei Ni, Masayoshi Tomizuka, and Ping Luo. Adaptdiffuser: Diffusion models as adaptive self-evolving planners. *arXiv preprint arXiv:2302.01877*, 2023.
- [74] Cong Lu, Philip Ball, Yee Whye Teh, and Jack Parker-Holder. Synthetic experience replay. *Advances in Neural Information Processing Systems*, 36, 2024.

- [75] Haoran He, Chenjia Bai, Kang Xu, Zhuoran Yang, Weinan Zhang, Dong Wang, Bin Zhao, and Xuelong Li. Diffusion model is an effective planner and data synthesizer for multi-task reinforcement learning. *Advances in neural information processing systems*, 36, 2024.
- [76] Eitan Altman. Constrained markov decision processes with total cost criteria: Lagrangian approach and dual linear program. *Mathematical methods of operations research*, 48(3):387–417, 1998.
- [77] Qian Lin, Chao Yu, Zongkai Liu, and Zifan Wu. Policy-regularized offline multi-objective reinforcement learning. *arXiv preprint arXiv:2401.02244*, 2024.
- [78] Scott Fujimoto and Shixiang Shane Gu. A minimalist approach to offline reinforcement learning. *Advances in neural information processing systems*, 34:20132–20145, 2021.
- [79] Zhang-Wei Hong, Pulkit Agrawal, Rémi Tachet des Combes, and Romain Laroche. Harnessing mixed offline reinforcement learning datasets via trajectory weighting. *arXiv preprint arXiv:2306.13085*, 2023.
- [80] Jonathan Ho, Ajay Jain, and Pieter Abbeel. Denoising diffusion probabilistic models. *Advances in neural information processing systems*, 33:6840–6851, 2020.
- [81] Jonathan Ho and Tim Salimans. Classifier-free diffusion guidance. *arXiv preprint arXiv:2207.12598*, 2022.
- [82] Tian Xu, Ziniu Li, and Yang Yu. Error bounds of imitating policies and environments. *Advances in Neural Information Processing Systems*, 33:15737–15749, 2020.
- [83] Zhepeng Cen, Zuxin Liu, Zitong Wang, Yihang Yao, Henry Lam, and Ding Zhao. Learning from sparse offline datasets via conservative density estimation. *arXiv preprint arXiv:2401.08819*, 2024.
- [84] Holden Lee, Jianfeng Lu, and Yixin Tan. Convergence for score-based generative modeling with polynomial complexity. *Advances in Neural Information Processing Systems*, 35:22870–22882, 2022.
- [85] Sitan Chen, Sinho Chewi, Jerry Li, Yuanzhi Li, Adil Salim, and Anru R Zhang. Sampling is as easy as learning the score: theory for diffusion models with minimal data assumptions. *arXiv preprint arXiv:2209.11215*, 2022.
- [86] Sven Gronauer. Bullet-safety-gym: Aframework for constrained reinforcement learning. 2022.
- [87] Zuxin Liu, Zijian Guo, Haohong Lin, Yihang Yao, Jiacheng Zhu, Zhepeng Cen, Hanjiang Hu, Wenhao Yu, Tingnan Zhang, Jie Tan, et al. Datasets and benchmarks for offline safe reinforcement learning. *arXiv preprint arXiv:2306.09303*, 2023.
- [88] Durk P Kingma, Shakir Mohamed, Danilo Jimenez Rezende, and Max Welling. Semi-supervised learning with deep generative models. *Advances in neural information processing systems*, 27, 2014.
- [89] Yang Song and Stefano Ermon. Generative modeling by estimating gradients of the data distribution. *Advances in neural information processing systems*, 32, 2019.
- [90] Prafulla Dhariwal and Alexander Nichol. Diffusion models beat gans on image synthesis. *Advances in neural information processing systems*, 34:8780–8794, 2021.
- [91] Alexander Quinn Nichol and Prafulla Dhariwal. Improved denoising diffusion probabilistic models. In *International conference on machine learning*, pages 8162–8171. PMLR, 2021.

Appendix

Table of Contents

A Proofs	15
A.1 Proof of Eq.(9)	15
A.2 Proof of Theorem 1	15
A.3 Proof of Theorem 2	16
B Supplementary experiments	17
B.1 Trajectory reweighting for distribution shaping	17
B.2 Supplementary CVAE data generation results	17
C Implementation details	17
C.1 Environment details	17
C.2 Dataset details	19
C.3 Algorithm details	20

A Proofs

A.1 Proof of Eq.(9)

By definition of the stationary state-action distribution,

$$|V_c^\pi(\mu_0) - V_c^*(\mu_0)| \quad (15)$$

$$= \frac{1}{1-\gamma} |\mathbb{E}_{(s,a) \sim d^\pi} [c(s,a)] - \mathbb{E}_{(s,a) \sim d^*} [c(s,a)]| \quad (16)$$

$$\leq \frac{C_{\max}}{1-\gamma} \sum_{s,a} |d^\pi(s,a) - d^*(s,a)| \quad (17)$$

$$= \frac{2C_{\max}}{1-\gamma} D_{\text{TV}}(d^\pi(s,a) \| d^*(s,a)) \quad (18)$$

$$\leq \frac{2C_{\max}}{1-\gamma} (D_{\text{TV}}(d^\pi(s,a) \| d^*(s)\pi(a|s)) + D_{\text{TV}}(d^*(s)\pi(a|s) \| d^*(s,a))) \quad (19)$$

$$= \frac{2C_{\max}}{1-\gamma} D_{\text{TV}}(d^\pi(s) \| d^*(s)) + \frac{2C_{\max}}{1-\gamma} \mathbb{E}_{d^*(s)} [D_{\text{TV}}(\pi(a|s) \| \pi^*(a|s))] \quad (20)$$

The second inequality holds by triangle inequality for total variation distance.

In general, the stationary distribution of learned policy is in between of the empirical distribution of offline data $d^\mathcal{D}$ and optimal d^* . Therefore, we can obtain

$$|V_c^\pi(\mu_0) - V_c^*(\mu_0)| \leq \frac{2C_{\max}}{1-\gamma} D_{\text{TV}}(d^*(s) \| d^\mathcal{D}(s)) + \frac{2C_{\max}}{1-\gamma} \mathbb{E}_{d^*(s)} [D_{\text{TV}}(\pi(a|s) \| \pi^*(a|s))]. \quad (21)$$

A.2 Proof of Theorem 1

Proof. By triangle inequality, we first decompose the TV distance between state-action distributions into a state distribution distance and a policy distance,

$$D_{\text{TV}}(d_g(s,a) \| d^*(s,a)) \quad (22)$$

$$= D_{\text{TV}}(d_g(s)\pi_g(a|s) \| d^*(s)\pi^*(a|s)) \quad (23)$$

$$\leq D_{\text{TV}}(d_g(s)\pi_g(a|s) \| d^*(s)\pi_g(a|s)) + D_{\text{TV}}(d^*(s)\pi_g(a|s) \| d^*(s)\pi^*(a|s)) \quad (24)$$

$$= D_{\text{TV}}(d_g(s) \| d^*(s)) + \mathbb{E}_{d^*(s)} [D_{\text{TV}}(\pi_g(a|s) \| \pi^*(a|s))] \quad (25)$$

We then consider two parts separately.

For the stationary state distribution distance, we suppose the optimal distribution $d^*(s)$ has a L -Lipschitz smooth score function and bounded second momentum. Meanwhile, note that the score function in Assumption 1 is closely related to the denoising model ϵ_θ [89, 90]:

$$\nabla_s \log d_g(s|\mathbf{y}) = -\frac{1}{\sqrt{1-\bar{\alpha}_t}} \epsilon_\theta(s|\mathbf{y}), \quad (26)$$

where $\epsilon_\theta(s|\mathbf{y})$ is the state marginal of the practical denoising model in Eq.(8). Therefore, by theorem 2 in [85], under Assumption 1, we have

$$D_{\text{TV}}(d_g(s)||d^*(s)) \lesssim \sqrt{D_{\text{KL}}(d^*(s)||\mathcal{N}(\mathbf{0}, \mathbf{I}^{|\mathcal{S}|}))} \exp(-K) + L(\sqrt{|\mathcal{S}|} + \mathbf{m}_2)\sqrt{K} + \epsilon_{\text{score}}\sqrt{K} \quad (27)$$

where K is the number of denoising timestep, $|\mathcal{S}|$ is the dimension of the state space, and \mathbf{m}_2 is the second momentum of $d^*(s)$. Therefore, aggregating the first two terms in RHS, we have

$$D_{\text{TV}}(d_g(s)||d^*(s)) \leq \tilde{\mathcal{O}}(\epsilon_{\text{score}}\sqrt{K}) + C(d^*(s), L, K), \quad (28)$$

where $C(\dots)$ is a constant w.r.t d^*, L, K .

Regarding the policy distance. By Pinsker's inequality,

$$D_{\text{TV}}(\pi_g(a|s)||\pi^*(a|s)) \leq \sqrt{\frac{1}{2}D_{\text{KL}}(\pi_g(a|s)||\pi^*(a|s))} \quad (29)$$

Meanwhile, since the action is generated by the inverse policy, i.e., $\pi_g = \hat{\pi}_{\text{inv}}$, by Assumption 2, we have

$$\mathbb{E}_{d^*(s)}[D_{\text{TV}}(\pi_g(a|s)||\pi^*(a|s))] \leq \mathbb{E}_{d^*(s)}\left[\sqrt{\frac{1}{2}D_{\text{KL}}(\pi_g(a|s)||\pi^*(a|s))}\right] \quad (30)$$

$$\leq \sqrt{\frac{1}{2}\mathbb{E}_{d^*(s)}[D_{\text{KL}}(\pi_g(a|s)||\pi^*(a|s))]} \quad (31)$$

$$= \sqrt{\epsilon_{\text{inv}}/2} \quad (32)$$

where the second inequality holds by Jensen's inequality.

Combining the Eq.(28) and Eq.(32), we finish the proof of theorem 1. \square

A.3 Proof of Theorem 2

We start from the Eq.(9). The policy distance can be further decomposed into

$$D_{\text{TV}}(\pi(a|s)||\pi^*(a|s)) \leq D_{\text{TV}}(\pi(a|s)||\pi^{\mathcal{D}}(a|s)) + D_{\text{TV}}(\pi^{\mathcal{D}}(a|s)||\pi^*(a|s)). \quad (33)$$

By Assumption 2 and 3 and Jensen's inequality, we have

$$\mathbb{E}_{d^*(s)}[D_{\text{TV}}(\pi(a|s)||\pi^*(a|s))] \quad (34)$$

$$\leq \mathbb{E}_{d^*(s)}[D_{\text{TV}}(\pi(a|s)||\pi^{\mathcal{D}}(a|s))] + \mathbb{E}_{d^*(s)}[D_{\text{TV}}(\pi^{\mathcal{D}}(a|s)||\pi^*(a|s))] \quad (35)$$

$$\leq \mathbb{E}_{d^*(s)}\left[\sqrt{D_{\text{KL}}(\pi(a|s)||\pi^{\mathcal{D}}(a|s))/2}\right] + \mathbb{E}_{d^*(s)}\left[\sqrt{D_{\text{KL}}(\pi^{\mathcal{D}}(a|s)||\pi^*(a|s))/2}\right] \quad (36)$$

$$\leq \sqrt{\mathbb{E}_{d^*(s)}[D_{\text{KL}}(\pi(a|s)||\pi^{\mathcal{D}}(a|s))]/2} + \sqrt{\mathbb{E}_{d^*(s)}[D_{\text{KL}}(\pi^{\mathcal{D}}(a|s)||\pi^*(a|s))]/2} \quad (37)$$

$$\leq \sqrt{\epsilon_{\text{reg}}/2} + \sqrt{\epsilon_{\text{inv}}/2} \quad (38)$$

Plug-in Eq.(28) and (38) into Eq.(21), we have

$$|V_c^\pi(\mu_0) - V_c^*(\mu_0)| \leq \frac{2C_{\text{max}}}{1-\gamma} \left(\tilde{\mathcal{O}}(\epsilon_{\text{score}}\sqrt{K}) + C(d^*(s), L, K) + \sqrt{\epsilon_{\text{inv}}/2} + \sqrt{\epsilon_{\text{reg}}/2} \right). \quad (39)$$

Meanwhile, notice that the optimal policy is constraint satisfactory, i.e.,

$$V_c^*(\mu_0) \leq \kappa. \quad (40)$$

Therefore, we have

$$V_c^\pi(\mu_0) - \kappa \leq \frac{2C_{\text{max}}}{1-\gamma} \left(\tilde{\mathcal{O}}(\epsilon_{\text{score}}\sqrt{K}) + C(d^*(s), L, K) + \sqrt{\epsilon_{\text{inv}}/2} + \sqrt{\epsilon_{\text{reg}}/2} \right), \quad (41)$$

which finishes the proof of Theorem 2.

B Supplementary experiments

B.1 Trajectory reweighting for distribution shaping

In this section, we provide details about the trajectory reweighting experiment presented in section 4.2. Following previous work [33, 79] in offline RL, we adopted datapoint reweighting in policy optimization, which can be formulated via importance sampling as:

$$\mathcal{J}_{\text{off}}^w(\pi, \lambda) \approx \mathbb{E}_{(s,a) \sim \mathcal{D}_w}[\mathcal{J}_{\text{off}}(\pi, \lambda)] = \mathbb{E}_{(s,a) \sim \mathcal{D}}[w(s, a)\mathcal{J}_{\text{off}}(\pi, \lambda)], \quad (42)$$

where $\mathcal{J}_{\text{off}}^w(\pi, \lambda)$ is the objective function after reweighting. In this experiment, we utilize a Boltzmann energy function as adopted in [33] for offline RL tasks:

$$w(\tau) \propto \exp(\alpha_1 R(\tau)^2 + \alpha_2 (C(\tau) - \kappa)^2) \quad (43)$$

Here $w(\tau)$ means that all the state-action pairs in one trajectory share the same weight, which is related to the cost and reward returns $C(\tau), R(\tau)$. We adopt $\alpha_1 = \alpha_2 = 1$ in the experiments shown in Figure 3.

B.2 Supplementary CVAE data generation results

Due to the page limit, we omit the visualization of reward and cost distribution using the CVAE method for data generation. Here we provide the results in Figure 8. From the reward performance and the cost performance, we can observe that CVAE can hardly encode conditions into the data reconstruction, leading to similar results when setting different conditions. From the trajectory reconstruction results shown in Figure 8(c), we can observe that the generated trajectories are almost the same as the original one. This feature is not desirable for our distribution shaping purpose. In contrast, our method OASIS can successfully shape the distribution as shown in Figure 7, with the strong capability of the diffusion model in the condition-guided denoising process.



Figure 8: CVAE reconstruction. (a) Reward performance of the generated data: $\mathbb{E}[r(s, a)], (s, a) \sim d_g$, (b) Cost performance of the generated data: $\mathbb{E}[c(s, a)], (s, a) \sim d_g$. In (a) and (b), the x-axis and y-axis mean the reward and cost conditions, and the value of both conditions and expectations are normalized to the same scale: $[0, 1]$; (c) The data reconstruction results using the condition $[0.1, 0.5]$ of 10 sampled trajectories in the dataset.

C Implementation details

C.1 Environment details

Due to the page limit, we omit some descriptions of experiments in the main context. Here we give the more details about our experiment tasks. Both the Circle task and the Run task are from a publicly available benchmark [86].

Circle tasks. The agents are rewarded for running along a circle boundary. The reward function is defined as:

$$r(s, a, s') = \frac{-yv_x + xv_y}{1 + \sqrt{x^2 + y^2 - radius}} + r_{\text{robot}}(s) \quad (44)$$

where x, y are the positions of the agent with state s' , v_x , and v_y are velocities of the agent with state s' . $radius$ is the radius of the circle area, and $r_{robot}(s_t)$ is the specific reward for different robot.

The agent gets cost when exceeding the boundaries. The cost function is defined as:

$$\text{Boundary: } c(s_t) = \mathbf{1}(|x| > x_{lim}) \quad (45)$$

where x_{lim} is the boundary position.

Run tasks. Agents are rewarded for running fast along one fixed direction and are given costs if they run across the boundaries or exceed a velocity limit. The reward function is defined as:

$$r(s, a, s') = \|\mathbf{x}_{t-1} - \mathbf{g}\|_2 - \|\mathbf{x}_t - \mathbf{g}\|_2 + r_{robot}(s_t) \quad (46)$$

The cost function is defined as:

$$c(s, a, s') = \max(1, \mathbf{1}(|y| > y_{lim}) + \mathbf{1}(\|\mathbf{v}_t\|_2 > v_{lim})) \quad (47)$$

where v_{lim} is the speed limit, and y_{lim} is the y position of the boundary, $\mathbf{v}_t = [v_x, v_y]$ is the velocity of the agent with state s' , $\mathbf{g} = [g_x, g_y]$ is the position of a virtual target, $\mathbf{x}_t = [x_t, y_t]$ is the position of the agent at timestamp t , \mathbf{x}_{t-1} is the Cartesian coordinates of the agent with state s , \mathbf{x}_t is the Cartesian coordinates of the agent with state s' , and $r_{robot}(s_t)$ is the specific reward for the robot.

Agents. We use three different robot agents in our experiments: Ball, Car, and Drone. The action space dimension, observation space dimension, and the timesteps for these six tasks are shown in Table. 3.

Table 3: Environment description

	Max timestep	Action space dimension	Observation space dimension
BallRun	100	2	7
CarRun	200	2	7
DroneRun	200	4	17
BallCircle	200	2	8
CarCircle	300	2	8
DroneCircle	300	4	18

C.2 Dataset details

We provide details about the dataset types we presented in the experiment part. The Full, Tempting, Conservative, and Hybrid datasets for Ball-Circle and Car-Circle tasks are shown in Figure 9, 10, respectively. All the Tempting datasets associated with results in Table 1 are shown in Figure 11.

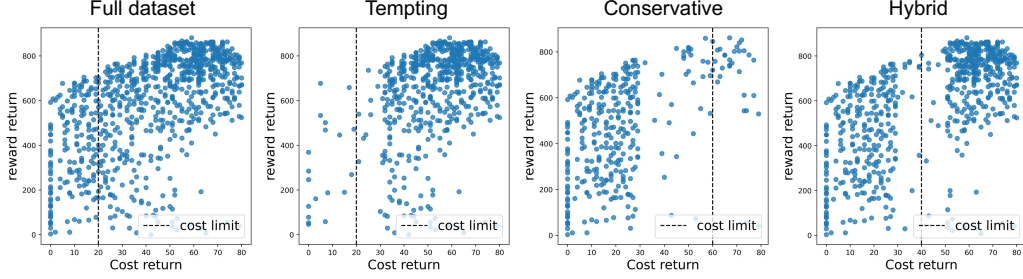


Figure 9: BallCircle Dataset types. Each point represents $(C(\tau), R(\tau))$ of a trajectory τ in the dataset.

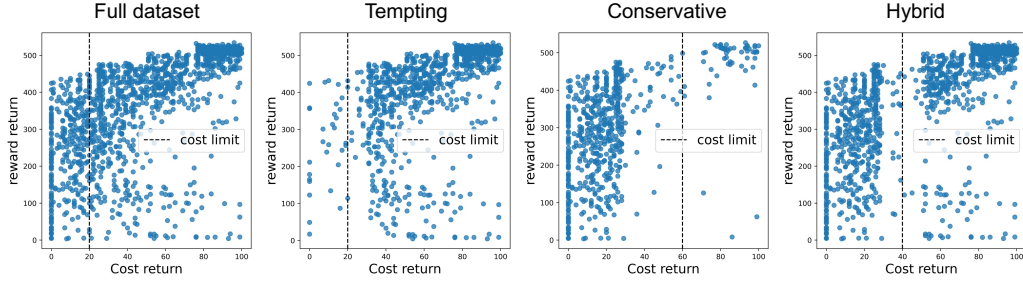


Figure 10: CarCircle Dataset types. Each point represents $(C(\tau), R(\tau))$ of a trajectory τ in the dataset.

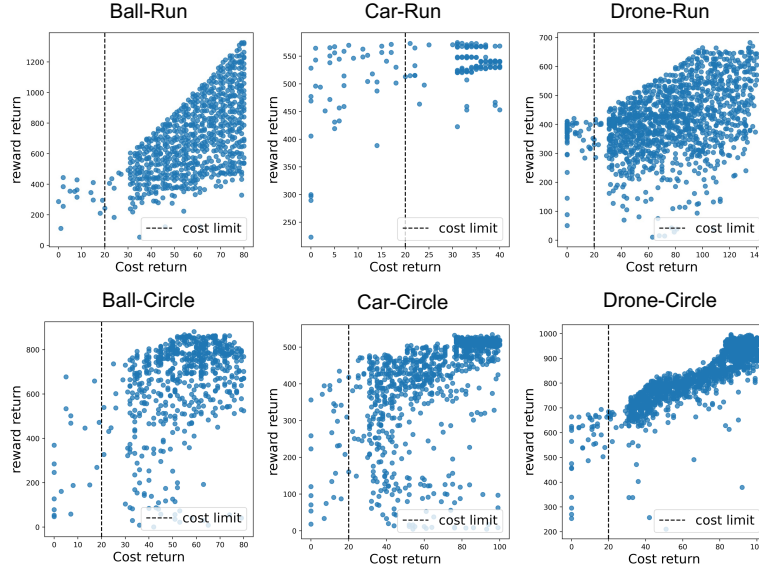


Figure 11: All tempting datasets. Each point represents $(C(\tau), R(\tau))$ of a trajectory τ in the dataset.

C.3 Algorithm details

OASIS algorithm training diagram In this work, we use the cosine β schedule [91] to calculate $\beta_t, t = 1, \dots, K$. Then we let $\alpha_t = 1 - \beta_t$, and $\bar{\alpha}_t = \prod_{i=1}^t \alpha_i$ and denote the state dimension as m . With these notations, we show the training process of the OASIS data generator for one epoch in Alg. 2.

Algorithm 2: OASIS (training)

- 1: **Input:** Original Dataset \mathcal{D} , predefined β_t and $\bar{\alpha}_t$, diffusion core $\epsilon_\theta(\mathbf{x}_k, \mathbf{y}, k)$, learning rate lr , loss function $L(\cdot, \cdot)$.
 - 2: **for** each sub-trajectory $\tau_i \in \mathcal{D}$ **do**
 - 3: Extract the states from τ_i : $\{(s_0, s_1, \dots, s_T)\} \# [T, m]$;
 - 4: Get the return conditions $\mathbf{y} = [C, R]$ associated with these sub-trajectories;
 - 5: With probability $p = 0.25$ to mask the condition information as: $\mathbf{y} \leftarrow \emptyset$
 - 6: Get Gaussian Noise $\text{noise} = \mathcal{N}(\mathbf{0}, \mathbf{I}) \# [T, m]$;
 - 7: Randomly sample time $t \in [0, \dots, K - 1]$;
 - 8: Calculate the forward sampling state $\mathbf{x}_{\text{noise}} = \bar{\alpha}_t * \tau_i + (1 - \bar{\alpha}_t) * \text{noise}$;
 - 9: Apply initial state condition $\mathbf{x}_{\text{noise}}[0] \leftarrow s_0$;
 - 10: Reconstruct noisy sub trajectory $\mathbf{x}_{\text{recon}} = \epsilon_\theta(\mathbf{x}_{\text{noise}}, \mathbf{y}, k)$;
 - 11: Minimize the reconstruction loss $\theta \leftarrow \theta - lr * \nabla_\theta L(\mathbf{x}_{\text{noise}}, \mathbf{x}_{\text{recon}})$;
 - 12: **end for**
 - 13: **Output:** Updated diffusion core $\epsilon_\theta(\mathbf{x}_k, \mathbf{y}, k)$;
-

Network and hyperparameter details. For the dynamics model \hat{p} , we utilize a MLP. For the denoising core, we utilize a U-net, which has also been used in previous works [73, 71]. The U-net is visualized in Figure 12. The hyperparameters for our method are summarized in Table 4. More details are available in the code.

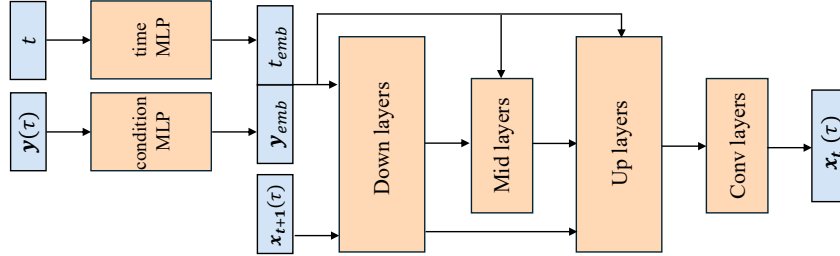


Figure 12: U-Net structure.

Baseline details. For the baseline methods BC, BCQ-Lag, BEAR-Lag, COptiDICE, CPQ, and CDT, we adopt the code base provided in the benchmark [87]. For the FISOR method, we use the code provided by the authors [29].

Computing resources. The experiments are run on a server with $2 \times$ AMD EPYC 7542 32-Core Processor CPU, $2 \times$ NVIDIA RTX A6000 graphics, and 252 GB memory. For one single experiment, OASIS takes about 4 hours with 200,000 steps to train the data generator. It takes about 1.5 hours to train a BCQ-Lag agent on this generated dataset for 200,000 steps.

Table 4: Hyperparameters	
Hyperparameters	Value
L (length of subsequence)	32
K (denoising timestep)	20
Batch size	256
Learning rate	3.0e-5
w_α	2.0